

Inertial Alfvén waves and acceleration of electrons in nonuniform magnetic fields

C. E. J. Watt,¹ R. Rankin,¹ I. J. Rae,¹ and D. M. Wright²

Received 27 September 2005; revised 2 December 2005; accepted 16 December 2005; published 31 January 2006.

[1] We present results from self-consistent simulations of the electron response to shear Alfvén pulses in the presence of non-uniform magnetic fields and the associated mirror force. We discuss how energies of resonantly accelerated beam particles are affected by the local phase velocity of the pulse, and show that time-of-flight models are inadequate for describing electron acceleration since the acceleration can occur at more than one location along the field line as the pulse propagates toward the ionosphere. We also demonstrate that electron conics in low-altitude satellite observations of electron acceleration can be explained in terms of field-aligned inertial Alfvén wave pulses, without the requirement of a static potential drop or a standing Alfvén wave structure. **Citation:** Watt, C. E. J., R. Rankin, I. J. Rae, and D. M. Wright (2006), Inertial Alfvén waves and acceleration of electrons in nonuniform magnetic fields, *Geophys. Res. Lett.*, 33, L02106, doi:10.1029/2005GL024779.

1. Introduction

[2] Previous work has shown that electrons can be accelerated along auroral field lines by either a quasi-static potential drop [e.g., *Evans, 1974*], or by kinetic or inertial shear Alfvén waves which propagate along the field, from altitudes of 4–5 R_E and above, toward the ionosphere [e.g., *Lysak, 1990*]. In this article, we focus on the self-consistent dynamic acceleration of electrons due to shear Alfvén waves in the inertial limit (i.e., those waves with perpendicular wavelength λ_{\perp} comparable to the electron skin depth $\delta_e = c/\omega_{pe}$, where c is the speed of light and ω_{pe} is the electron plasma frequency) in the presence of a non-uniform ambient magnetic field. In the inertial limit, Alfvén waves are known to support a parallel electric field E_{\parallel} that can accelerate electrons in the field-aligned direction, although more study is required into the details of this interaction.

[3] It is well established that Alfvénic perturbations on auroral or cusp field lines are associated with field-aligned electron acceleration [*Yamauchi et al., 2001; Andersson et al., 2002; Chaston et al., 2002; Su et al., 2004; Tanaka et al., 2005a*]. These observations have inspired a number of models to explain various details of the plasma and field measurements. In order to understand and quantify the acceleration process, some authors have used a single- or multi-fluid model for the waves, with 1-D test-particle

analysis for the electron dynamics [*Thompson and Lysak, 1996; Chaston et al., 2000; Su et al., 2004; Tanaka et al., 2005b*]. Other studies have used a single-fluid model for the waves, with 1-D Liouville mapping used for the electron dynamics [*Kletzing, 1994; Kletzing and Hu, 2001*]. Successful as these models have been, they do not describe wave-particle interactions self-consistently. In some cases, static potential drops must be assumed in addition to wave acceleration processes, and constraints on the density and temperature profiles must be imposed in order to reproduce observations.

[4] Recently, a self-consistent Vlasov-kinetic model has been developed to examine the electron response to inertial shear Alfvén waves (ISAW) [*Watt et al., 2004*]. In a uniform magnetic field, i.e., neglecting the mirror force, this model has successfully reproduced field-aligned electron acceleration signatures from the Fast Auroral SnapshoT (FAST) spacecraft [*Watt et al., 2005*] with no constraints required for the plasma and field parameters along the field line. Furthermore, it was shown that enhancements in the low-energy electron energy flux, often known as suprathermal electron bursts, are signatures of current-carrying electrons required by the wave that are locally accelerated and decelerated as the wave passes over the plasma. They do not necessarily have to be trapped by the wave and carried through the plasma, as previously asserted [*Su et al., 2004*].

[5] The present study extends the work of *Watt et al.* [2004, 2005], by removing the constraint of uniform plasma and field along auroral field lines. The geomagnetic field is far from uniform, neither are the plasma parameters along the field line [e.g., *Kletzing et al., 1998*], and there may exist a static potential drop [*Evans, 1974*]. Non-uniformities in ambient magnetic field B_0 , number density n , temperature T and static potential Φ_0 all modify the acceleration of electrons by ISAW. In this paper, we isolate the effects of the non-uniform magnetic field and present an explanation for ISAW electron acceleration signatures seen in satellite data.

2. Simulation Code

[6] We model the electron-ISAW interaction using a drift-kinetic Vlasov simulation code which follows the electron dynamics along the field line. There are three simulation variables: the electric scalar potential $\phi(z)$, the parallel component of the magnetic vector potential $A_{\parallel}(z)$, and the electron distribution function $f_e(z, \mu, p_{\parallel})$, where z is the spatial coordinate along the field line, $\mu = m_e v_{\perp}^2 / (2B_0)$ is the magnetic moment, assumed to be conserved, v_{\perp} is the perpendicular component of the electron velocity, and $p_{\parallel} = v_{\parallel} + (q_e/m_e)A_{\parallel}$ is the parallel canonical momentum per unit mass. The three equations which move the simulation

¹Department of Physics, University of Alberta, Edmonton, Alberta, Canada.

²Radio and Space Plasma Physics Group, University of Leicester, Leicester, UK.

parameters forward in time and the boundary conditions on the potentials are discussed by *Watt et al.* [2004].

[7] The one-dimensional simulation domain extends between 800 km and $2.5 R_E$ altitude above the Earth, and we work under the assumption that B_0 is approximately dipolar and intersects Earth's surface at a latitude of 65° . Plasma in a non-uniform B_0 is subject to two forces: the mirror force $F_M = -\mu(\partial B_0/\partial z)$ that acts on particles with non-zero v_\perp , retarding and/or pushing them away from lower altitudes, and the parallel force $F_\parallel = q_e E_\parallel$ due to the wave E_\parallel , which can act in either direction and affects all of the electron distribution. In previous work using a uniform B_0 [*Watt et al.*, 2004, 2005], it was assumed that only electrons experience forces in the parallel direction, since they carry the parallel current J_\parallel due to the wave. However, with the introduction of a non-uniform B_0 , ions with non-zero v_\perp will also experience a small but finite F_M in the parallel direction, and so it is necessary to take this into account. Prior to launching an ISAW pulse into the simulation domain, a simulation is performed for both electrons and protons, using a kinetic equation for both species, until it reaches an equilibrium state. For this equilibrium calculation, the entire simulation domain is initialised with Maxwellian distribution functions with zero drift velocity for both species in v_\parallel and v_\perp (which is transformed into the coordinates μ and p_\parallel). Under the action of the mirror force, the distribution functions, f_e and f_i , evolve such that both electrons and ions develop non-zero contributions to J_\parallel . At each boundary, the incoming f_e and f_i are Maxwellian with fixed n and T . The drift velocity of the incoming ions v_{di} is set to zero, since it is assumed that any J_\parallel is largely carried by the electrons. The v_{de} of the incoming electrons is set to be consistent with any finite J_\parallel (due to non-zero A_\parallel) required at the boundary. Once the simulation has reached equilibrium, these contributions cancel such that $J_\parallel \sim 0$.

[8] Once the equilibrium has been reached, the proton response is switched off, and only the contributions to the zeroth and first moment of f_i are retained for use in the vector potential calculation. It is assumed that the protons will not respond significantly to the ISAW potentials.

3. Simulation Results

[9] To model the electron-ISAW interaction, we add a Gaussian-shaped potential pulse $\phi_0(t)$ to the scalar potential at the top boundary and allow it to propagate down the simulation domain. This form of pulse results in an initially bipolar, symmetrical E_\parallel which evolves self-consistently as it interacts with the plasma. The number density $n_e = 1.5 \times 10^7 \text{ m}^{-3}$ and temperature $T_e = 10 \text{ eV}$ are kept constant. These values are chosen to be a compromise since in the lower magnetosphere above the auroral oval, the plasma can vary between cold ($0.1\text{--}1.0\text{ eV}$) and dense ($n_e \sim 10^8 \text{ m}^{-3}$) at low altitudes [*Kletzing et al.*, 1998] to hot (10s or 100s of eV) and sparse ($n_e \sim 10^5$ or 10^6 m^{-3}) at higher altitudes. The discussion of the effect of varying n and T is avoided here for expediency. At the lower boundary, λ_\perp is set to 1 km, and the perpendicular wavenumber $k_\perp \propto B_0^{1/2}$ along the field line [*Chaston et al.*, 2002].

[10] Figure 1 shows the evolution of the differential electron energy flux of the downgoing field-aligned electrons ($v_\perp = 0, v_\parallel < 0$) at 4 different locations in the upper part

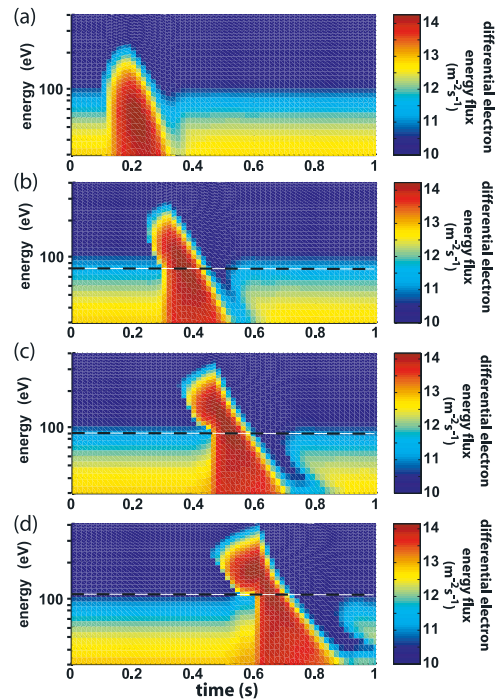


Figure 1. Differential electron energy flux of the downgoing electrons as a function of time from different locations in the drift-kinetic simulation code: (a) $z = 2.41 R_E$, (b) $z = 2.28 R_E$, (c) $z = 2.15 R_E$ and (d) $z = 2.02 R_E$. Dashed lines indicate K_{\min} .

of the simulation domain: (Figure 1a) $z = 2.41$, (Figure 1b) $z = 2.28$, (Figure 1c) $z = 2.15$, and (Figure 1d) $z = 2.02 R_E$ during times close to the launch of the scalar potential pulse (at $t = 0$). Figure 1a shows that near the top of the simulation, no resonantly accelerated electron beam has yet been formed. The strong enhancement in electron flux for all energies $\leq 200 \text{ eV}$ for $0.14 < t < 0.33 \text{ s}$ is due to the large J_\parallel associated with the ISAW. However, as the pulse propagates further down the simulation domain, a beam of resonantly accelerated electrons is formed which arrives before the pulse and its associated electron parallel current signature. Figure 1 shows that the lowest energy of electrons in the beam increases as the beam propagates down the field line. At $z = 2.28 R_E$, the lowest beam energy is $K_{\min} \sim 80 \text{ eV}$ (dashed line), increasing to $K_{\min} \sim 90 \text{ eV}$ at $z = 2.16 R_E$ and reaching $K_{\min} \sim 105 \text{ eV}$ at $z = 2.02 R_E$. This increase in K_{\min} is due to the increasing pulse phase velocity v_{ph} as it moves down the simulation domain (since the Alfvén speed increases as the pulse moves into an area of increasing magnetic field). At each location, the resonantly accelerated electrons are accelerated to velocities $v \geq v_{ph}$ [*Kletzing*, 1994; *Watt et al.*, 2005] through one-interaction Fermi acceleration. These resonantly accelerated electrons stream ahead of the pulse down the simulation domain, but the slowest beam electrons are caught up by the pulse at lower altitudes as v_{ph} increases, and are accelerated again.

[11] Since some of the electrons in the beam are accelerated at more than one location along the simulation domain, this may present a straightforward explanation for why simple time-of-flight analyses do not always uniquely determine a single source location for the accelerated

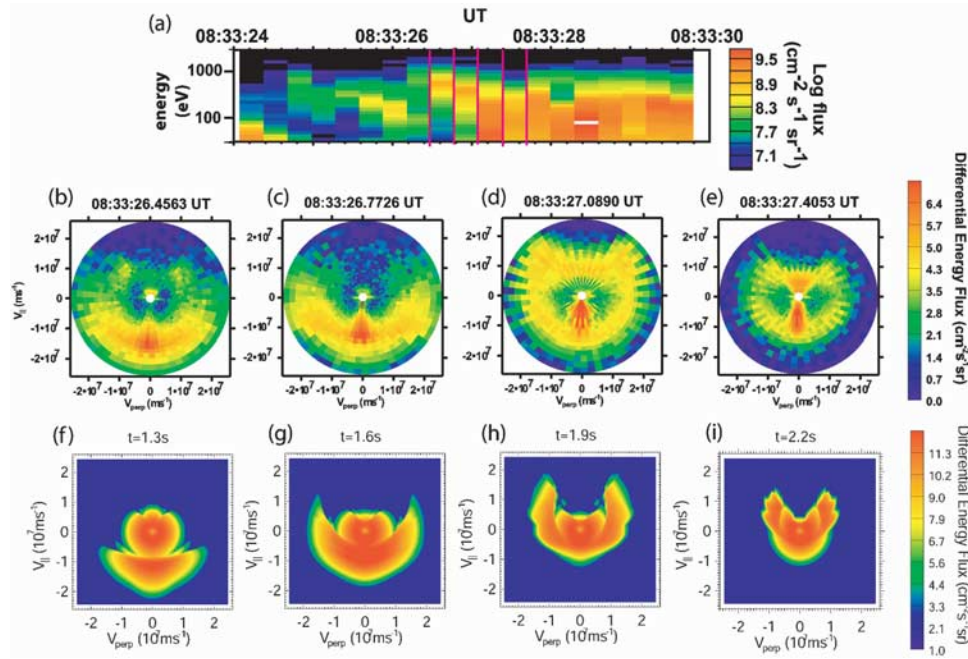


Figure 2. Comparison between FAST observations of an electron acceleration event during orbit 3568 and the results from the simulation code. (a) Differential electron energy flux of the downgoing electrons; (b, c, d, e) full two-dimensional plots of FAST differential electron energy flux as a function of v_{\parallel} and v_{\perp} for time intervals indicated with red vertical lines in Figure 2a; (f, g, h, i) two-dimensional plots of differential energy flux as a function of v_{\parallel} and v_{\perp} at $z = 0.5 R_E$ for time intervals of 0.3 s duration taken from the simulation. In the simulation, the field-aligned burst of low-energy electrons occurs at $t = 1.9$ s.

electrons [e.g., *Andersson et al., 2002; Tanaka et al., 2005a*]. We will investigate the full evolution of the beam electrons using a particle-tracing analysis in a future publication.

4. Data Comparison

[12] Observations of electron acceleration events associated with ISAWs also show specific signatures in the pitch-angle dependence of the accelerated electrons [where pitch-angle $\alpha = \tan^{-1}(v_{\perp}/v_{\parallel})$]. Here, we compare the α -dependence of the simulation electron energy flux with the FAST observations (not possible for the uniform simulations of *Watt et al. [2004, 2005]*).

[13] Figure 2 shows electron energy data from FAST orbit 3568 on 17th July 1997 (see *Watt et al. [2005]* for more details of this interval). Figure 2a shows the downgoing electron differential energy flux (where downgoing is defined as those electrons with $|\alpha| < 30^\circ$). There is an energy-dispersed beam signature in the electrons from 26.45–27.09s (times are defined in seconds after 0833 UT), which is followed immediately by a burst of field-aligned electrons for all energies below the lowest beam energy.

[14] Figures 2b–2e show the differential energy flux as a function of perpendicular and parallel velocity. The lower half of each panel corresponds to downgoing energy flux, whereas the top half corresponds to upgoing energy flux. Each of these four panels corresponds to one of the consecutive time intervals indicated with red lines in Figure 2a: (Figure 2b) 26.46–26.77s (when high-energy beam electrons arrive at the spacecraft); (Figure 2c) 26.77–27.09s (when the lower-energy beam electrons arrive at the spacecraft); (Figure 2d) 27.09–27.41s (during

the initial part of the field-aligned burst); (Figure 2e) 27.41–27.73s (continuation of the field-aligned burst). The beam electrons exhibit a wide spread in pitch-angle which increases as lower energy beam electrons reach the spacecraft [cf. *Andersson et al., 2002*]. Coincident with the strong burst of field-aligned electrons in Figure 2d, there is evidence of a much smaller flux of upgoing electrons at wide pitch-angles, a signature often referred to as an electron conic [*André and Eliasson, 1994; Eliasson et al., 1996*]. As the burst signature continues, the energies of the electrons forming the conic signature decrease, as can be seen in Figure 2e.

[15] Figures 2f–2i show the differential energy flux as a function of v_{\parallel} and v_{\perp} from the simulation described in section 3. All four plots are obtained at the location $z = 0.5 R_E$ in the simulation domain, and show the averaged differential energy flux for different time intervals relative to the start of the field-aligned electron burst at $t = 1.9$ s (the arrival of the pulse at that particular location): (Figure 2f) 1.3–1.6s, (Figure 2g) 1.6–1.9s, (Figure 2h) 1.9–2.2s and (Figure 2i) 2.2–2.5s.

[16] The simulation clearly shows the same wide-angle electron beam (Figure 2f), which becomes wider as time progresses and the beam energies decrease (Figure 2g). At the same time as the field-aligned burst of electrons, there is also a smaller flux of upgoing electrons at wide pitch-angles forming an electron conic signature (Figure 2h). The energies of the electrons forming the conic signature decrease during the burst (Figure 2i).

[17] The electrons in the simulation have an initial temperature of 10eV and so the background distribution function appears much broader in the simulation than in the

data. The temperature of the ambient plasma at the location of the FAST satellite (~ 3200 km altitude) during this interval is likely to be much colder, and so we see little evidence of the bulk plasma distribution function in the observations (Figures 2b–2e).

[18] Using the simulation results as a guide, we postulate a very simple explanation for the electron conic. The pulse resonantly accelerated a group of electrons at some height above the spacecraft. Some of those accelerated electrons will have nonzero v_{\perp} , and hence will be influenced by the mirror force F_M . The magnetic moment of each electron is conserved, and so for each electron, F_M will vary only with the magnitude of the local magnetic field gradient. The force which keeps the electrons streaming ahead of the pulse is the force due to the parallel electric field F_{\parallel} , which, upon studying the simulation results, does not change magnitude significantly during the propagation of the pulse down the field line. In this case, there is then a height at which $F_M > F_{\parallel}$ for those accelerated electrons with large v_{\perp} and they are slowed then returned back up the field line. As the beam of accelerated electrons travels to lower altitudes, electrons with smaller values of v_{\perp} will satisfy the condition $F_M > F_{\parallel}$ and will also be returned, hence the energies of electrons in the conic signature will be reduced. Only an ISAW pulse of short λ_{\perp} is required to explain these observations; there is no particular need to consider static potential drops or standing waves in the ionospheric Alfvén resonator [e.g., Thompson and Lysak, 1996].

5. Summary

[19] We have shown, via a self-consistent drift-kinetic simulation, the dynamic response of electrons to a shear Alfvén wave of short perpendicular scale length. Electrons experiencing resonant acceleration due to the parallel electric field of an ISAW may be accelerated at more than one location by the same wave as it propagates through an increasing Alfvén speed gradient. This may be the reason why a simple time-of-flight analysis of energy-dispersed electron signatures does not always yield a single location for the acceleration mechanism.

[20] We have also shown that the electron conic signatures sometimes associated with electron acceleration events are a natural consequence of the acceleration due to the ISAW. The wave parallel electric field pushes the resonant electron beam ahead of it down the field line until it reaches a location where the mirror force overcomes the parallel electric field force for beam electrons with large v_{\perp} . At lower altitudes, where the magnetic field gradient is even larger, beam electrons with smaller values of v_{\perp} will also experience a change in the force balance, and will be accelerated upwards.

[21] We will investigate the details of the accelerated electron trajectories and the self-consistent dependence of the acceleration on plasma and wave parameters in future publications.

[22] **Acknowledgments.** This work was supported by NSERC and the Canadian Space Agency in Canada. D. M. W. is supported by a PPARC Advanced Research Fellowship. The authors are very grateful to C. W. Carlson and the rest of the FAST team for the use of FAST data. C. E. J. W. would like to thank E. Sumbur of the AICT Research Support Group at the University of Alberta for help with parallelization of the simulation code. This research has been enabled by the use of WestGrid computing resources, which are funded in part by the Canada Foundation for Innovation, Alberta Innovation and Science, BC Advanced Education, and the participating research institutions. Westgrid equipment is provided by IBM, Hewlett Packard and SGI.

References

- Andersson, L., N. Ivchenko, J. H. Clemmons, A. A. Namgaladze, B. Gustavsson, J.-E. Wahlund, L. Eliasson, and R. Yu. Yurik (2002), Electron signatures and Alfvén waves, *J. Geophys. Res.*, *107*(A9), 1244, doi:10.1029/2001JA900096.
- André, M., and L. Eliasson (1994), Some electron conic generation mechanisms, in *Space Plasmas: Coupling Between Small and Medium Scale Processes*, *Geophys. Monogr. Ser.*, vol. 86, edited by M. Ashour-Abdalla, T. Chang, and P. Dusenbery, pp. 61–72, AGU, Washington, D. C.
- Chaston, C. C., C. W. Carlson, R. E. Ergun, and J. P. McFadden (2000), Alfvén waves, density cavities and electron acceleration observed from the FAST spacecraft, *Phys. Scr.*, *784*, 64.
- Chaston, C. C., J. W. Bonnell, L. M. Peticolas, C. W. Carlson, and J. P. McFadden (2002), Driven Alfvén waves and electron acceleration: A FAST case study, *Geophys. Res. Lett.*, *29*(11), 1535, doi:10.1029/2001GL013842.
- Eliasson, L., M. André, R. Lundin, R. Potelette, G. Marklund, and G. Holmgren (1996), Observations of electron conics by the Viking satellite, *J. Geophys. Res.*, *101*, 13,225.
- Evans, D. S. (1974), Precipitating electron fluxes formed by a magnetic field aligned potential difference, *J. Geophys. Res.*, *79*, 2853.
- Kletzing, C. A. (1994), Electron acceleration by kinetic Alfvén waves, *J. Geophys. Res.*, *99*, 11,095.
- Kletzing, C. A., and S. Hu (2001), Alfvén wave generated electron time dispersion, *Geophys. Res. Lett.*, *28*, 693.
- Kletzing, C. A., F. S. Mozer, and R. B. Torbert (1998), Electron temperature and density at high latitude, *J. Geophys. Res.*, *103*, 14,837.
- Lysak, R. L. (1990), Electrodynamic coupling of the magnetosphere and ionosphere, *Space Sci. Rev.*, *52*, 33.
- Su, Y.-J., S. T. Jones, R. E. Ergun, and S. E. Parker (2004), Modeling of field-aligned electron bursts by dispersive Alfvén waves in the dayside auroral region, *J. Geophys. Res.*, *109*, A11201, doi:10.1029/2003JA010344.
- Tanaka, H., Y. Saito, K. Asamura, S. Ishii, and T. Mukai (2005a), High time resolution measurements of multiple electron precipitations with energy-time dispersion in high-latitude part of the cusp region, *J. Geophys. Res.*, *110*, A12208, doi:10.1029/2004JA010644.
- Tanaka, H., Y. Saito, K. Asamura, and T. Mukai (2005b), Numerical modeling of electron energy-time dispersions in the high-latitude part of the cusp region, *J. Geophys. Res.*, *110*, A05213, doi:10.1029/2004JA010665.
- Thompson, B. J., and R. L. Lysak (1996), Electron acceleration by inertial Alfvén waves, *J. Geophys. Res.*, *101*, 5359.
- Watt, C. E. J., R. Rankin, and R. Marchand (2004), Kinetic simulations of electron response to shear Alfvén waves in magnetospheric plasmas, *Phys. Plasmas*, *11*, 1277.
- Watt, C. E. J., R. Rankin, I. J. Rae, and D. M. Wright (2005), Self-consistent electron acceleration due to inertial Alfvén wave pulses, *J. Geophys. Res.*, *110*, A10S07, doi:10.1029/2004JA010877.
- Yamauchi, M., L. Andersson, P. A. Lindqvist, S. Ohtani, J. H. Clemmons, J.-E. Wahlund, L. Eliasson, and R. Lundin (2001), Acceleration signatures in the dayside boundary layer and the cusp, *Phys. Chem. Earth*, *26*, 195.
- I. J. Rae, R. Rankin, and C. E. J. Watt, Department of Physics, University of Alberta, 412 Avadh Bhatia Physics Laboratory, Edmonton, Canada AB T6G 0T1. (cwatt@space.ualberta.ca)
- D. M. Wright, Radio and Space Plasma Physics Group, University of Leicester, Leicester, UK.